Original Article

Fluorofenidone enhances cisplatin efficacy in non-small cell lung cancer: a novel approach to inhibiting cancer progression

Shunjun Wang[1,2,3#], Guowei Liu[4#], Laishun Yu[5#], Chenzi Zhang[6#], Fabrizio Marcucci[7], Yupeng Jiang[2]^

[1]Department of Cardiology Surgery, Xiangya Hospital of Central South University, Changsha, China; [2]Department of Oncology, The Second Xiangya Hospital, Central South University, Changsha, China; [3]School of Medical Imaging, Changsha Medical University, Changsha, China; [4]Department of Thoracic Surgery, Qinghai Provincial People's Hospital, Xining, China; [5]Department of Respiratory and Critical Care Medicine, Qinghai Provincial People's Hospital, Xining, China; [6]Department of Hematology, Xiangya Hospital of Central South University, Changsha, China; [7]Department of Pharmacological and Biomolecular Sciences, University of Milan, Milan, Italy

Contributions: (I) Conception and design: Y Jiang, S Wang; (II) Administrative support: Y Jiang, G Liu; (III) Provision of study materials or patients: Y Jiang, G Liu, L Yu; (IV) Collection and assembly of data: S Wang, C Zhang; (V) Data analysis and interpretation: Y Jiang, S Wang; (VI) Manuscript writing: All authors; (VII) Final approval of manuscript: All authors.

[#]These authors contributed equally to this work.

Correspondence to: Yupeng Jiang, PhD, MD. Department of Oncology, The Second Xiangya Hospital, Central South University, No. 139 Renmin Road, Changsha 410011, China. Email: jiangyupeng0717@csu.edu.cn.

Background: Non-small cell lung cancer (NSCLC), the most prevalent lung cancer subtype, presents significant treatment challenges. Cisplatin (CP)-based regimens are central to the treatment of multiple solid tumors, but its use is restricted due to its dose-related renal toxicity. We previously found that fluorofenidone {1-[3-fluorophenyl]-5-methyl-2-[(1H)]-pyridone (AKF-PD)} effectively reverses CP-induced acute kidney injury (AKI). However, it remains unclear whether AKF-PD can synergistically ameliorate NSCLC when used together with CP. Thus, this study sought to investigate the effect of AKF-PD on NSCLC and examined its combinatory use with CP for cancer treatment.

Methods: We conducted cell viability assays, 5-ethynyl-2'-deoxyuridine (EdU) experiments, colony-forming assays, wound-healing tests, and Transwell experiments in A549 and H1299 cells to explore the effects of AKF-PD on NSCLC. We then detected the epithelial-mesenchymal transition (EMT) markers [i.e., epithelial cadherin (E-cadherin), matrix metallopeptidase 9 (MMP9), vimentin, and snail family transcriptional repressor 1 (SNAIL)], phosphoinositide 3-kinase (PI3K)/protein kinase B (AKT)/mechanistic target of rapamycin (mTOR), and mitogen-activated protein kinase (MAPK), to identify the potential mechanisms of AKF-PD. Further, via the combined use of AKF-PD and CP, we found that AKF-PD enhanced the antitumor effect of CP, and we suggest that this may be due to its inhibitory effect on EMT. We also examined the effect of combining AKF-PD and CP in other cancer cell lines, including Hela, SiHA, MDA-MB-231, 5-8F, and UM-UC-3 cells.

Results: AKF-PD significantly inhibited the proliferation and invasion of NSCLC cells (A549 and H1299), suppressed the activation of the MAPK and PI3K/AKT/mTOR pathways, and inhibited the EMT of the tumor cells. When AKF-PD was used in combination with CP, these effects were further enhanced. We also found that AKF-PD enhanced the anti-cancer effect of CP in a variety of cancer cell lines, including cervical cancer (Hela cells and SiHA cells), nasopharyngeal cancer (5-8F cells), triple-negative breast cancer (MDA-MB-231 cells), and bladder cancer (UM-UC-3 cells).

Conclusions: AKF-PD not only mitigates CP-induced AKI but also enhances the anti-cancer efficacy of CP. Our findings provide valuable insights into the treatment of NSCLC and may have clinical applications.

^ ORCID: 0000-0001-8971-2079.

Keywords: Non-small cell lung cancer (NSCLC); fluorofenidone (AKF-PD); cisplatin (CP); epithelial-mesenchymal transition (EMT)

Submitted Sep 07, 2024. Accepted for publication Nov 04, 2024. Published online Nov 27, 2024.
doi: 10.21037/tlcr-24-811
View this article at: https://dx.doi.org/10.21037/tlcr-24-811

Introduction

Non-small cell lung cancer (NSCLC) is the most common type of lung cancer, and accounts for approximately 85% of all lung cancer cases (1). The 2-year survival rate of NSCLC has increased in recent years as a result of advances in diagnosis and treatment; however, NSCLC remains the leading cause of cancer-related deaths (2,3).

Cisplatin (CP) is a widely available, cheap, and potent platinum-based drug used for the treatment of multiple solid tumors, including NSCLC (4). Although targeted therapies have shown remarkable success in NSCLC patients with driver mutations, such as epidermal growth factor receptor (EGFR) exon 19 deletions and exon 21 L858R mutations, more than 50% of NSCLC patients still require CP-based regimens as the first-line treatment (5). However, the adverse effects of CP on the kidneys have limited its development and use (6). Several clinical attempts have been made to ameliorate CP-induced acute kidney injury (AKI), including the use of saline hydration. However, treatment outcomes remain unsatisfactory (7). Additionally, these procedures may further weaken the anti-cancer activity of CP (8).

Fluorofenidone {1-[3-fluorophenyl]-5-methyl-2-[(1H)]-pyridone (AKF-PD)} (Figure S1) is a novel low-molecular-weight pyridone agent (MW =203.91 g/mol) (9). AKF-PD was initially considered a broad-spectrum anti-organ fibrosis drug and has been shown to have high efficacy in various models of liver, kidney, and pulmonary fibrosis (10-13). Recently, studies have reported that the correlation and pathogenic similarities between fibrosis and cancer development in multiple organs are similar to those between idiopathic pulmonary fibrosis and hepatitis virus-induced liver fibrosis (14-16). The fibrotic tissue surrounding the tumor can facilitate tumor metastasis, and the tumor itself can also recruit fibroblasts; Hence, the cross-talk between tumor and fibrosis might be a fundamental process in cancer progression (17). Notably, AKF-PD can also ameliorate CP-induced AKI *in vivo* and *in vitro* (18). These studies strongly suggest that AKF-PD could be used in combination with CP in cancer treatment. However, it remains unknown whether AKF-PD has direct antitumor effects and whether these effects can modulate the antitumor activity of CP. In this article we report results that have been obtained in investigating this possibility. We present this article in accordance with the ARRIVE reporting checklist (available at https://tlcr.amegroups.com/article/view/10.21037/tlcr-24-811/rc).

Highlight box

Key findings

- A novel treatment that combines fluorofenidone {1-[3-fluorophenyl]-5-methyl-2-[(1H)]-pyridone (AKF-PD)} with cisplatin (CP) may be a better choice of non-small cell lung cancer (NSCLC).

What is known, and what is new?

- Previous studies have shown that AKF-PD can ameliorate CP-induced acute kidney injury and multi-organ fibrosis.
- We administered AKF-PD with CP and found that this regimen further enhanced the effect of CP in the treatment of NSCLC. Thus, this is a promising treatment method for NSCLC, which may not only enhance the treatment effects, but may also decrease the treatment side effects.

What is the implication, and what should change now?

- CP remains a critical first-line treatment for NSCLC. However, this study has identified a potential detoxification and efficacy enhancing treatment measure that may change the future clinical medication pattern, which may especially benefit patients with poor kidney function.
- This study was mainly conducted using mice and cell lines; thus, further clinical trials on humans need to be conducted to enable this discovery to be applied in clinical practice.

Methods

Materials

NSCLC cells (A549 and H1299), cervical carcinoma cells (Hela and SiHa), nasopharyngeal cancer cells (5-8F), triple-negative breast cancer cells (MDA-MB-231), bladder cancer cells (UM-UC-3), and proximal renal

tubule cells (NRK-52E) were provided by Shanghai Cell Bank (Chinese Academy of Sciences), Shanghai, China. Lewis cells (C7205) were purchased from Beyotime (Shanghai, China). AKF-PD (20150516) was synthesized by Haikou Pharmaceutical Company (Haikou, China). CP (HY-17394) was obtained from Sigma Aldrich (St. Louis, MO, USA). Vimentin (#5741), epithelial cadherin (E-cadherin) (#3195), phosphorylated-c-Jun N-terminal kinase (p-JNK) (#4668), phosphorylated-extracellular signal-regulated kinase 1/2 (p-ERK1/2) (#4370), p-P38 (#4511), phosphorylated-protein kinase B (p-AKT) (#4060), phosphorylated-mechanistic target of rapamycin (p-mTOR) (#5536), mTOR (#2983), phosphoinositide 3-kinase (PI3K) (#4257), JNK (#9252), ERK1/2 (#4695), P38 (#8690), AKT (#4685), and glyceraldehyde-3-phosphate dehydrogenase (GAPDH) (#9211) were purchased from Cell Signaling Technology (Danvers, MA, USA). P-PI3K (ab18265) and matrix metallopeptidase 9 (MMP9) (ab38898) antibodies were purchased from Abcam Company (Cambridge, UK). Snail family transcriptional repressor 1 (SNAIL) (PA5-114645) was purchased from Thermo Fisher Scientific (Bartlesville, OK, USA). N-cadherin (66219-1-lg) was obtained from Proteintech (Wuhan, China). Phosphate-buffered saline (PBS) solution was obtained from Sigma Aldrich. Fetal bovine serum (FBS) was obtained from Invitrogen. Dimethyl sulfoxide (DMSO), the Cell Counting Kit-8 (CCK-8) assay kit, and the 5-ethynyl-2'-deoxyuridine (EdU) kit were purchased from Beyotime. Transwell Chamber and Matrigel Matrix Glue were purchased from Corning (Tewksbury, MA, USA). All other chemicals were of analytical grade.

Animal experiments

Animal experiments were performed under a project license (No. 20220493) granted by the Experimental Animal Ethics Committee of the Second Xiangya Hospital of Central South University, in compliance with the Second Xiangya Hospital guidelines for the care and use of animals. A protocol was prepared before the study without registration. C57 mice (aged 5 weeks; 16–18 g) were obtained from the Silaike Laboratory (Shanghai, China). The mice were fed with standard food in a controlled environment (21±2 ℃, 50%±10% relative humidity, and 12 h of light; a maximum of four mice were housed per cage). Before starting the experiment, the animals underwent a week of acclimation to the new environment. Then, 5×10^5 Lewis lung cancer cells were subcutaneously injected into the axillary region of the mice. The mice were assigned to the following four groups: control, AKF-PD, CP, and CP + AKF-PD. After 1 week, the mice in the control group were injected with saline and saline gavage; the CP and CP + AKF-PD group mice were injected intraperitoneally with 5 mg/kg CP per week; and the AKF-PD and AKF-PD + CP group mice were treated by gavage with 400 mg/kg/d AKF-PD [dissolved in a vehicle solvent of 0.5% sodium carboxymethyl cellulose (CMCNa)]. All mice were euthanized after 3 weeks, and the subcutaneous tumors were collected.

Cell cultures

The cell cultures were maintained in RPMI 1640 complete medium and incubated at 37 ℃ under a 5% carbon dioxide (CO_2) atmosphere. The cell cultures were treated with 100 units/mL of penicillin and 100 μg/mL of streptomycin. NSCLC cells were treated with different concentrations of CP or AKF-PD according to the experimental conditions for at least 3 times.

Cell viability assays

Cells at logarithmic growth stage were collected and digested with trypsin, and the concentration of the cell suspension was adjusted to 5×10^4 cells/mL. Briefly, 100 μL of cell suspension was added to each well of a 96-well plate, and at least five parallel wells were set. After treatment for 24 h, the supernatant was replaced with CCK-8 reagent, and then further incubated for 30 min at 37 ℃. The absorbance at 450 nm was detected using a microplate reader, and the inhibitory rate of tumor cell proliferation and 50% effective concentration (EC_{50}) was calculated.

EdU cell proliferation staining

EdU cell proliferation staining was performed using an EdU kit. Briefly, A549 or H1299 cells (2×10^4 cells/well) were seeded in 24-well plates. Subsequently, cells were incubated with EdU for 3 h, fixed with 4% paraformaldehyde for 15 min, and permeabilized using 0.3% Triton X-100 for another 15 min. Then, cells were incubated with the Click Reaction Mixture for 30 min at room temperature in the dark and then incubated with Hoechst 33342 for 10 min. The EdU-positive cells were identified under a fluorescence microscope, and quantified by counting the percentage of EdU-positive nuclei in five random fields per well to determine the percentage of proliferating cells.

Colony-forming assays

Briefly, cells were added to each well of a 96-well plate. The cells were plated and then treated with different concentrations of AKF-PD [0, 200 μg/mL (0.98 mM), 400 μg/mL (1.97 mM), and 800 μg/mL (3.94 mM)] with or without CP (1 μM). Finally, each well was fixed with methanol for 30 min and stained with crystal violet for 30 min. The number of cell clones was counted using a scanner.

Wound-healing tests

Wound-healing tests were performed to assess the cell migration ability. The cells were inoculated into six-well plates. After performing the wound-healing tests, the cells were treated with 0% FBS-containing medium and different concentrations of AKF-PD solution [0, 200 μg/mL (0.98 mM), 400 μg/mL (1.97 mM), and 800 μg/mL (3.94 mM)]. At 0, 12, and 24 h, photographs of the cells were taken, and the cells were counted.

Transwell experiments

To assess the invasive potential of cells, the upper chamber of Transwell supports was first coated with substrate glue diluted in serum-free medium at a 1:8 ratio. The cells were then digested and seeded into the upper chamber in 0% FBS-containing medium and supplemented with varying concentrations of AKF-PD [0, 200 μg/mL (0.98 mM), 400 μg/mL (1.97 mM), and 800 μg/mL (3.94 mM)] and/or CP (10 μM). The lower chamber was filled with 20% FBS-containing medium. After 24 h, the cells were fixed with methanol for 30 min and stained with crystal violet for 30 min for subsequent counting.

Immunohistochemistry

The tumor sections were dewaxed and rehydrated, and then treated with H_2O_2 (3%) for 20 min. Next, they were treated with pepsin (0.4%) for 20 min before treatment with bovine serum albumin (5%) in PBS for 30 min. The sections were incubated at 4 ℃ overnight with an anti-N-cadherin antibody. Afterwards, the samples were washed in PBS and incubated with secondary antibodies. The results were visualized by diaminobenzidine staining. ImageJ software was used to highlight and quantify the immunostaining signals. Positive staining areas were quantified as a percentage of the whole area.

Western blotting

Proteins were isolated using a nuclear/cytosol fractionation kit (Thermo Fisher Scientific). Equal amounts of lysate protein were separated via 8–15% sodium dodecyl sulfate-polyacrylamide gel electrophoresis and transferred to polyvinylidene difluoride membranes. The membranes were blocked in 5% skim milk and then incubated with primary antibodies at a 1:1,000 dilution at 4 ℃ overnight. Target proteins were detected using the enhanced chemiluminescence method (Bio-Rad, Hercules, CA, USA). Signal detection was performed using an ImageQuant LAS 500 Imaging System (GE Healthcare, Life Sciences, Seongnam, Korea).

Statistical analysis

SPSS 21.0 software (IBM, Armonk, NY, USA) was used for the statistical analysis. The experimental results are presented as the mean ± standard deviation. The comparisons between two groups were performed using the *t*-test, and the comparisons between multiple groups were performed using a one-way analysis of variance. A P value <0.05 was considered statistically significant.

Results

AKF-PD inhibited the proliferation and colony-forming ability of NSCLC cells

To assess the effect of AKF-PD on NSCLC cell lines (A549 and H1299), cells were treated with varying concentrations of AKF-PD, and cell proliferation was evaluated with the CCK-8 assay. The inhibitory effect of 400 and 800 μg/mL of AKF-PD on cell proliferation was significant (P<0.0001). While 200 μg/mL of AKF-PD inhibited the proliferation of A549 cells (P<0.05), the effect on H1299 cells was not significant (P>0.05) (*Figure 1A*,*1B*). The EC_{50} of AKF-PD on A549 cells was 1,030 μg/mL and 1,118 μg/mL for H1299 cells (*Figure 1C*,*1D*). Also, EdU experiments showed that the inhibitory effect of 400 and 800 μg/mL of AKF-PD on cell proliferation was significant (P<0.05), but not that of 200 μg/mL (*Figure 1E-1H*). Moreover, colony formation experiments showed that increasing the concentration of AKF-PD had a significant inhibitory effect (*Figure 1I*). Overall, these experiments show that AKF-PD treatment

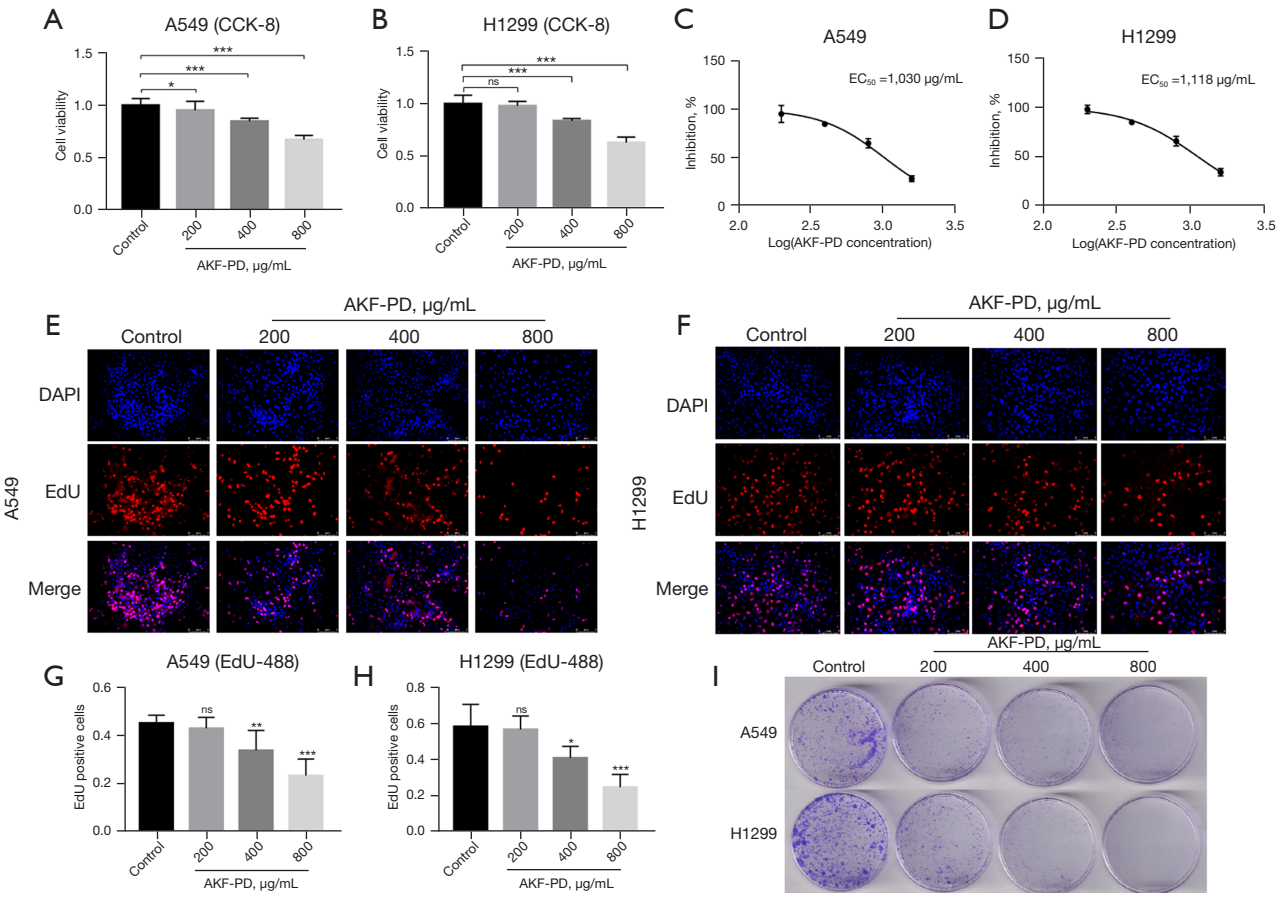

Figure 1 AKF-PD reduces the proliferation and colony-forming ability of NSCLC cells. The lung cancer cell lines were treated with different concentrations of AKF-PD for 24 h. (A,B) Cell viability was determined by CCK-8 assay, and (C,D) the EC_{50} values of AKF-PD were calculated. (E-H) The proliferation of the A549 and H1299 cells was detected by EdU-488; magnification: 200×. (I) The effects of AKF-PD in NSCLC were examined by colony-forming assay of NSCLC; staining: crystal violet. *, P<0.05; **, P<0.01; ***, P<0.001; and ns, P>0.05. CCK-8, Cell Counting Kit-8; AKF-PD, fluorofenidone; EC_{50}, 50% effective concentration; DAPI, 4'-6-diamidino-2-phenylindole; EdU, 5-ethynyl-2'-deoxyuridine; NSCLC, non-small cell lung cancer.

inhibited proliferation of NSCLC cells.

AKF-PD inhibited the invasion of NSCLC cells

The wound-healing assays showed that after 12 h of treatment, the migration of the cells in the control group (the A549 and H1299 cells) was significantly higher than that of the treatment groups. Cell migration in the AKF-PD-treated groups was inhibited at a dose of 200 μg/mL of AKF-PD (P<0.05 and <0.0001 for 200 and >200 μg/mL, respectively). At 24 h, the trend was similar to that observed at 12 h, but inhibition was further increased. Thus, the effect of AKF-PD was both dose- and time-dependent. Additionally, there was no significant difference in the wound-healing rates between the A549 and H1299 cells treated with 400 and 800 μg/mL of AKF-PD (*Figure 2A-2D*). In the Transwell invasion experiments, the inhibitory effect of AKF-PD was dose-dependent significantly decreased compared to the control group (P<0.05) (*Figure 2E-2G*). These results show that AKF-PD inhibits tumor cell migration and invasion.

AKF-PD inhibited epithelial-mesenchymal transition (EMT) in NSCLC cells

EMT is a key process in cancer proliferation, migration, and invasion (19,20). Several EMT-associated markers were evaluated to examine a possible effect of AKF-PD on

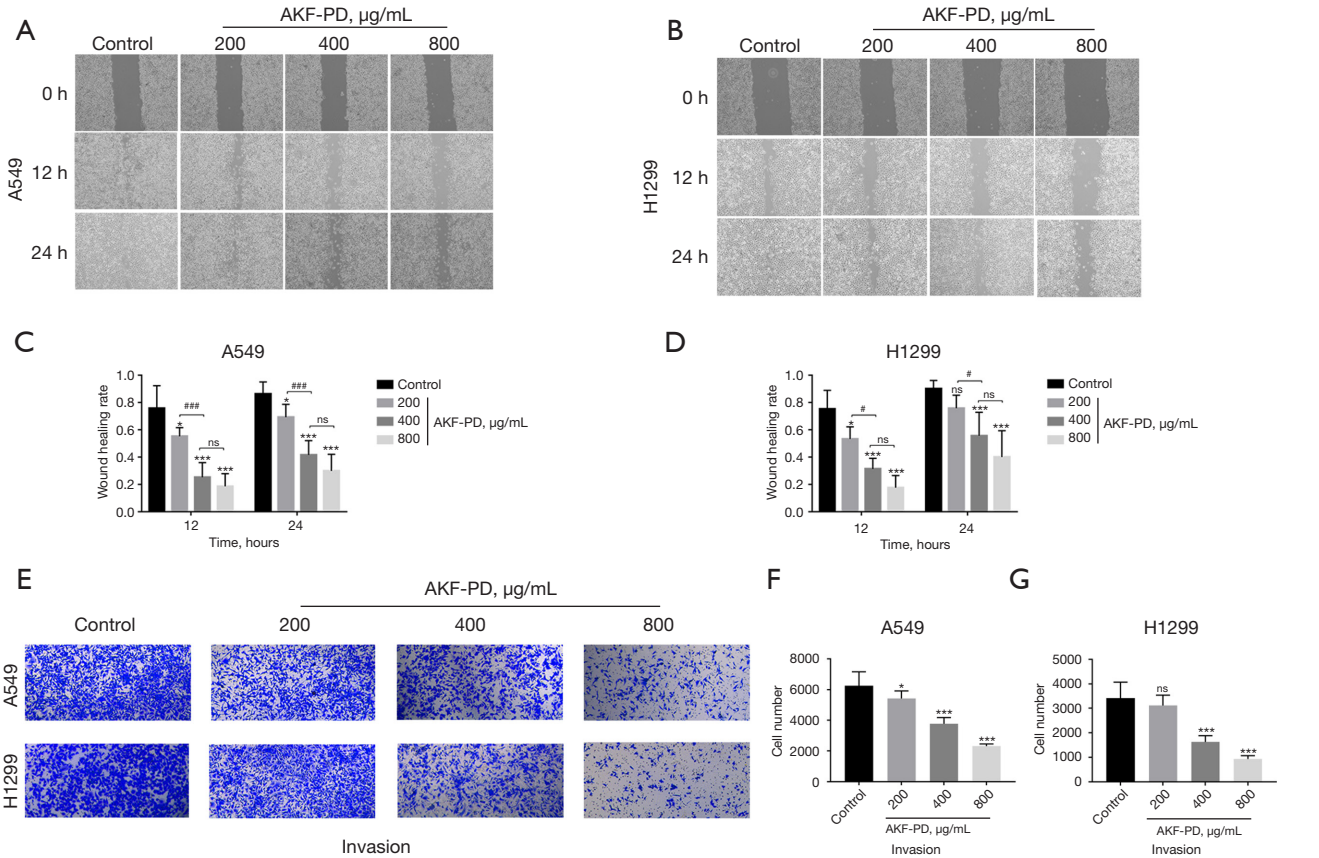

Figure 2 AKF-PD inhibits migration and invasion in NSCLC cells. (A-D) The wound-healing rate of the A549 and H1299 cells under the influence of different concentrations of AKF-PD was detected by scratch test; magnification: 200×. (E-G) The effects of different concentrations of AKF-PD on invasion in the two types of cells were examined by Transwell assay; magnification: 200×; staining: crystal violet. *, P<0.05; ***, P<0.001; #, P<0.05; ###, P<0.001; and ns, P>0.05. AKF-PD, fluorofenidone; NSCLC, non-small cell lung cancer.

the EMT of NSCLC. The expression of E-cadherin, an epithelial marker of A549 and H1299 cells, was significantly increased in AKF-PD-treated cells (P<0.05). In A549 and H1299 cells, AKF-PD treatment significantly decreased the expression of MMP9, vimentin, and SNAIL compared to the control group (P<0.05) (*Figure 3*). These results show that AKF-PD treatment inhibited EMT in NSCLC cells.

AKF-PD inhibited the activation of the PI3K/AKT/mTOR and mitogen-activated protein kinase (MAPK) pathways in NSCLC cells

PI3K/AKT/mTOR and MAPK are signaling pathways that play crucial roles in the tumorigenesis of many cancer types (21,22). Here, we found that AKF-PD suppresses the phosphorylation of JNK, ERK, and P38 in both A549 and H1299 cells (*Figure 4A-4D*). As to the PI3K/AKT/mTOR pathway, we found a notable decrease in p-PI3K, p-AKT, and p-mTOR levels after AKF-PD treatment in A549 and H1299 cells (*Figure 4E-4H*).

AKF-PD in combination with CP resulted in increased inhibition of the proliferation of NSCLC cells

Recently, we reported that AKF-PD significantly ameliorates CP-induced AKI *in vivo* and *in vitro* (18). However, the effect of AKF-PD on the anti-NSCLC activity of CP remained unclear. Therefore, we investigated the effect of combined treatment with AKF-PD and CP in NSCLC cells. First, different concentrations of CP were used to treat A549 and H1299 cells. CP significantly inhibited the proliferation of NSCLC cells (P<0.05) (*Figure 5A,5B*). When treatment was performed with AKF-PD in combination with CP, 200 μg/mL of AKF-PD did not significantly

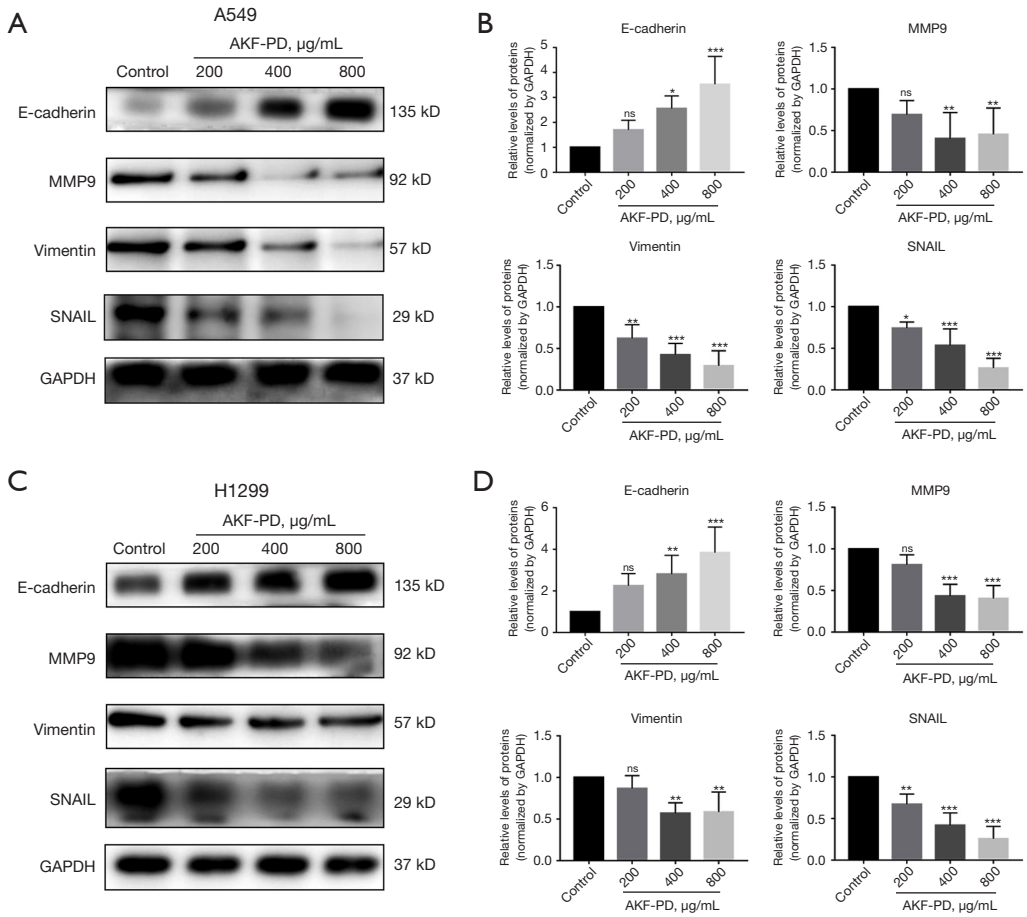

Figure 3 AKF-PD inhibits EMT in NSCLC cells. (A,B) The western blot analysis and quantitative data of E-cadherin, MMP9, vimentin, and SNAIL in A549. (C,D) The western blot analysis and quantitative data of E-cadherin, MMP9, vimentin, and SNAIL in H1299. *, P<0.05; **, P<0.01; ***, P<0.001; and ns, P>0.05. AKF-PD, fluorofenidone; E-cadherin, epithelial cadherin; MMP9, matrix metallopeptidase 9; SNAIL, snail family transcriptional repressor 1; GAPDH, glyceraldehyde-3-phosphate dehydrogenase; EMT, epithelial-mesenchymal transition; NSCLC, non-small cell lung cancer.

affect H1299 cell viability, while doses >400 μg/mL significantly reduced the viability of A549 and H1299 cells (*Figure 5C,5D*).

The EC_{50} values for CP in A549 and H1299 cells, were 18.21 and 20.4 μM, respectively (*Figure 5E,5F*). The EC_{50} values for AKF-PD in the presence of 10 μM CP were 700.8 μg/mL for the A549 cells and 836.1 μg/mL for the H1299 cells (*Figure 5G,5H*). Notably, these values were lower than those obtained when AKF-PD was used alone.

The EdU proliferation experiments showed that the combined AKF-PD and CP treatment inhibited proliferation of A549 and H1299 cells (P<0.05) (*Figure 5I-5L*). The cell colony-forming assays showed that the inhibitory effect of CP combined with AKF-PD was greater than that of the individual compounds (*Figure 5M*).

Additionally, our flow cytometry analysis using fluorescein isothiocyanate (FITC)/propidium iodide (PI) staining revealed that AKF-PD did not significantly impact apoptosis induced by CP in NSCLC cells, partially suggesting that the aforementioned effect may not be related to apoptosis (Figure S2).

For *in vivo* experiments we used an AKF-PD dose of 400 mg/kg/d since our previous study had shown that 400 μg/mL is the maximum dose of AKF-PD that can be used without damaging normal cells (23). We found a significant reduction in the size and weight of tumors in mice treated with CP and AKF-PD (P<0.05), suggesting that therapeutic effect of the CP and AKF-PD combination

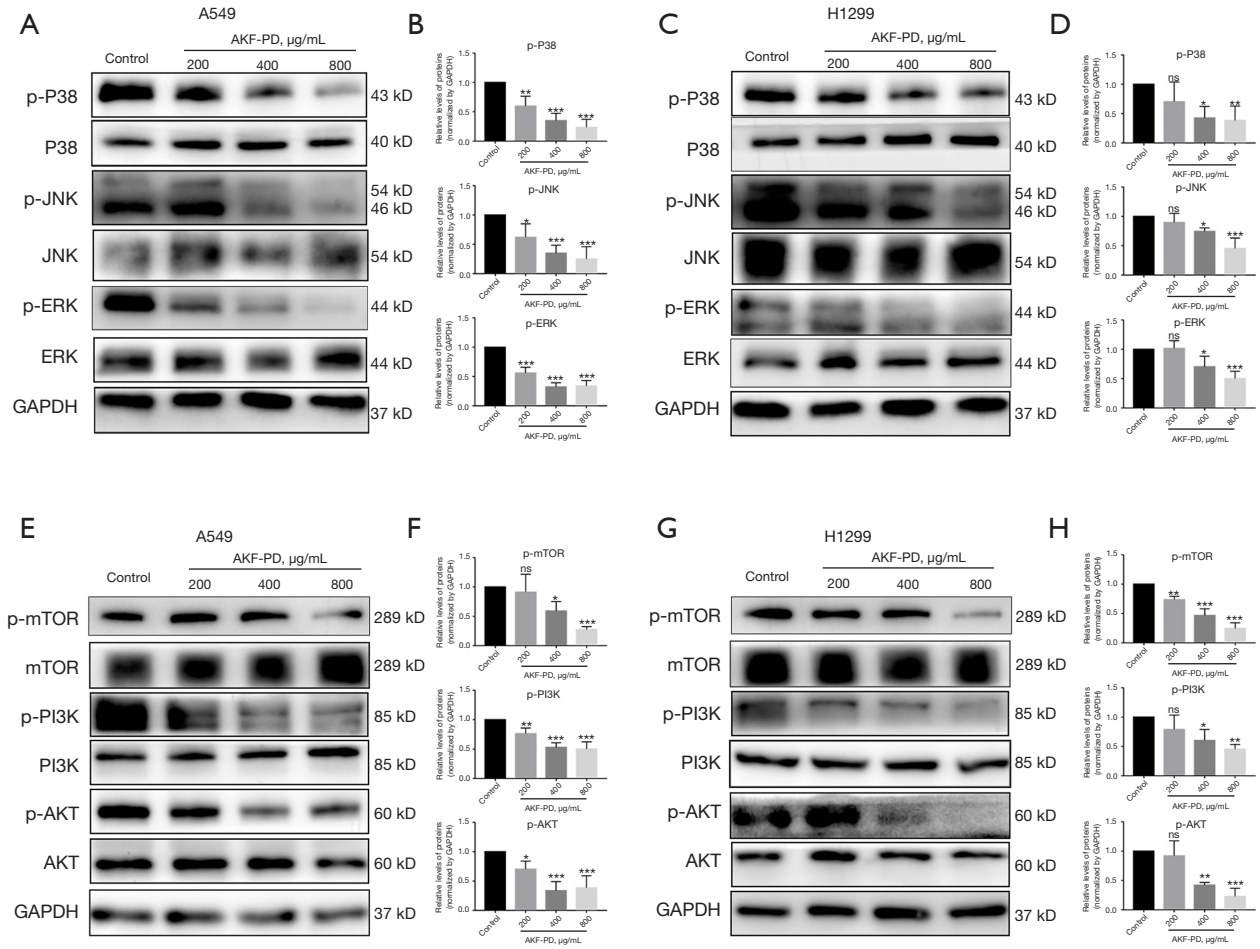

Figure 4 AKF-PD inhibits the activation PI3K/AKT/mTOR and MAPK in NSCLC cells. (A-D) The expression of p-P38, p-JNK, and p-ERK in (A,B) A549 and (C,D) H1299 was examined by western blot assay. (E-H) The expression of p-mTOR, p-PI3K, and p-AKT in (E,F) A549 and (G,H) H1299 was examined by western blot assay. *, P<0.05; **, P<0.01; ***, P<0.001; and ns, P>0.05. AKF-PD, fluorofenidone; p-, phosphorylated; JNK, c-Jun N-terminal kinase; ERK, extracellular signal-regulated kinase; GAPDH, glyceraldehyde-3-phosphate dehydrogenase; mTOR, mechanistic target of rapamycin; PI3K, phosphoinositide 3-kinase; AKT, protein kinase B; MAPK, mitogen-activated protein kinase; NSCLC, non-small cell lung cancer.

was superior to that of either drug alone (P<0.05) (*Figure 5N-5P*). These results showed that in terms of inhibiting tumor growth, the dual-drug combination for the treatment of NSCLC providing increased growth inhibition compared to individual compounds.

AKF-PD in combination with CP increased the inhibition of the invasion and migration of NSCLC cells

To determine whether AKF-PD in combination with CP inhibits cell migration and invasion, we conducted wound-healing and Transwell invasion experiments. The combination of CP and AKF-PD further reduced both the migration and invasion of the NSCLC cells as compared to the individual compounds (*Figure 6*).

AKF-PD in combination with CP increased the EMT inhibition of NSCLC cells

In the following study, we investigated the anti-EMT properties of the AFK-PD/CP combination and found that, compared to the individual compounds, the combination regimens had a more pronounced effect on decreasing the expression of SNAIL, vimentin, and N-cadherin, while

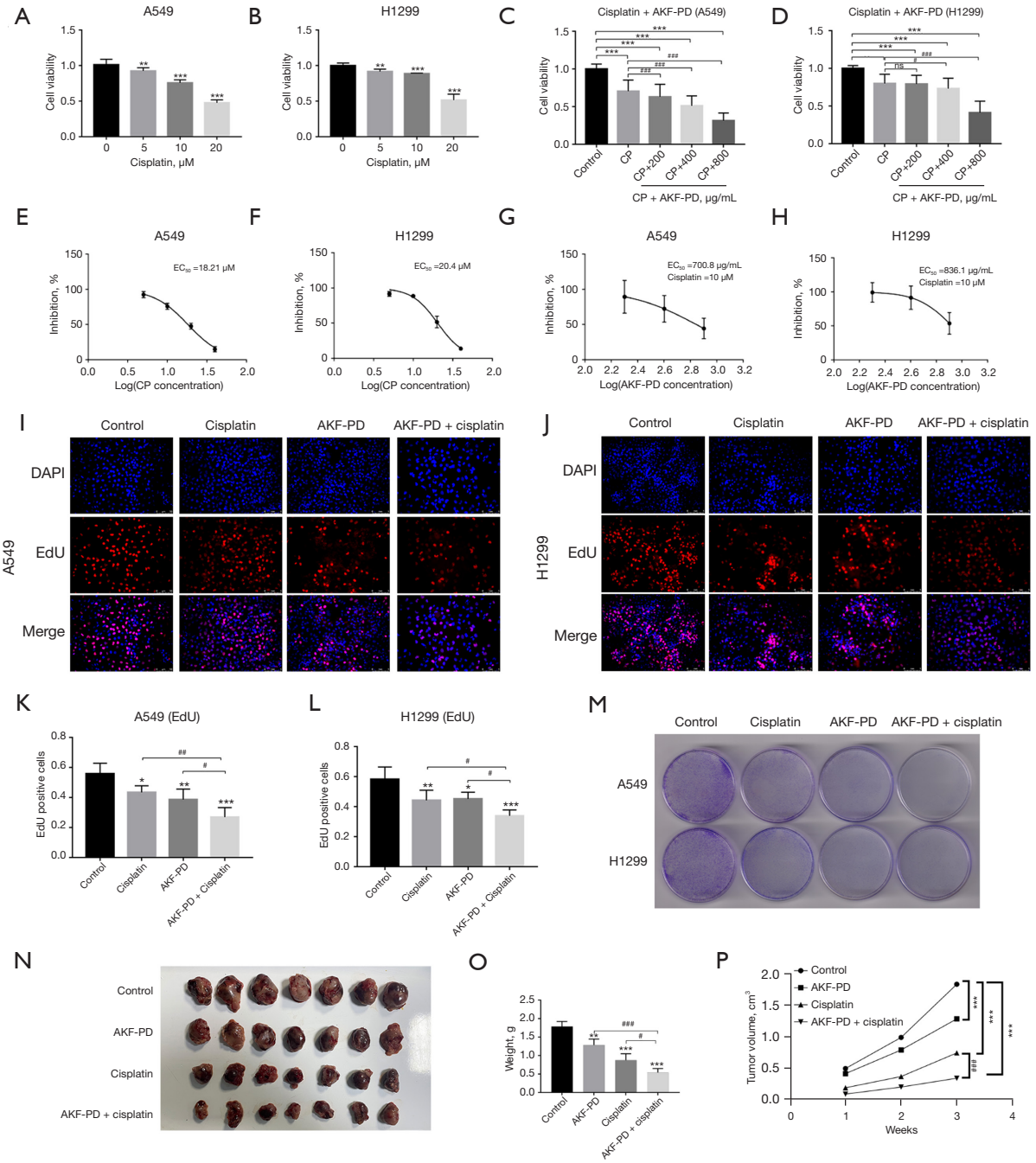

Figure 5 AKF-PD combined with CP further inhibited the proliferation of NSCLC cells. (A,B) Cell viability was determined by CCK-8 assay after treating the A549 and H1299 cells with various concentrations of CP (0, 5, 10, and 20 μm) for 24 h. (C,D) The inhibitory effects of combining CP (10 μm) with various concentrations of AKF-PD (200, 400, or 800 μg/mL) on (C) A549 and (D) H1299 cells was determined by CCK-8 assay. (E-H) The EC50 values of AKF-PD under the stimulation of CP (10 μm) in A549 and H1299 were evaluated. (I-L) The proliferation of the A549 and H1299 cells treated with CP and/or AKF-PD was detected by EdU; magnification: 200×. (M) The effects of CP (1 μm) and AKF-PD (400 μg/mL) on NSCLC was determined by colony-forming assay of NSCLC; staining: crystal violet. (N-P) The effects of AKF-PD (400 mg/kg/d) and/or CP (5 mg/kg) treatment on (N) tumorigenesis, (O) tumor weight, and (P) tumor volume in Lewis cells in mice. *, P<0.05; **, P<0.01; ***, P<0.001; #, P<0.05; ##, P<0.01; ###, P<0.001; and ns, P>0.05. AKF-PD, fluorofenidone; CP, cisplatin; EC50, 50% effective concentration; DAPI, 4'-6-diamidino-2-phenylindole; EdU, 5-ethynyl-2'-deoxyuridine; NSCLC, non-small cell lung cancer; CCK-8, Cell Counting Kit-8.

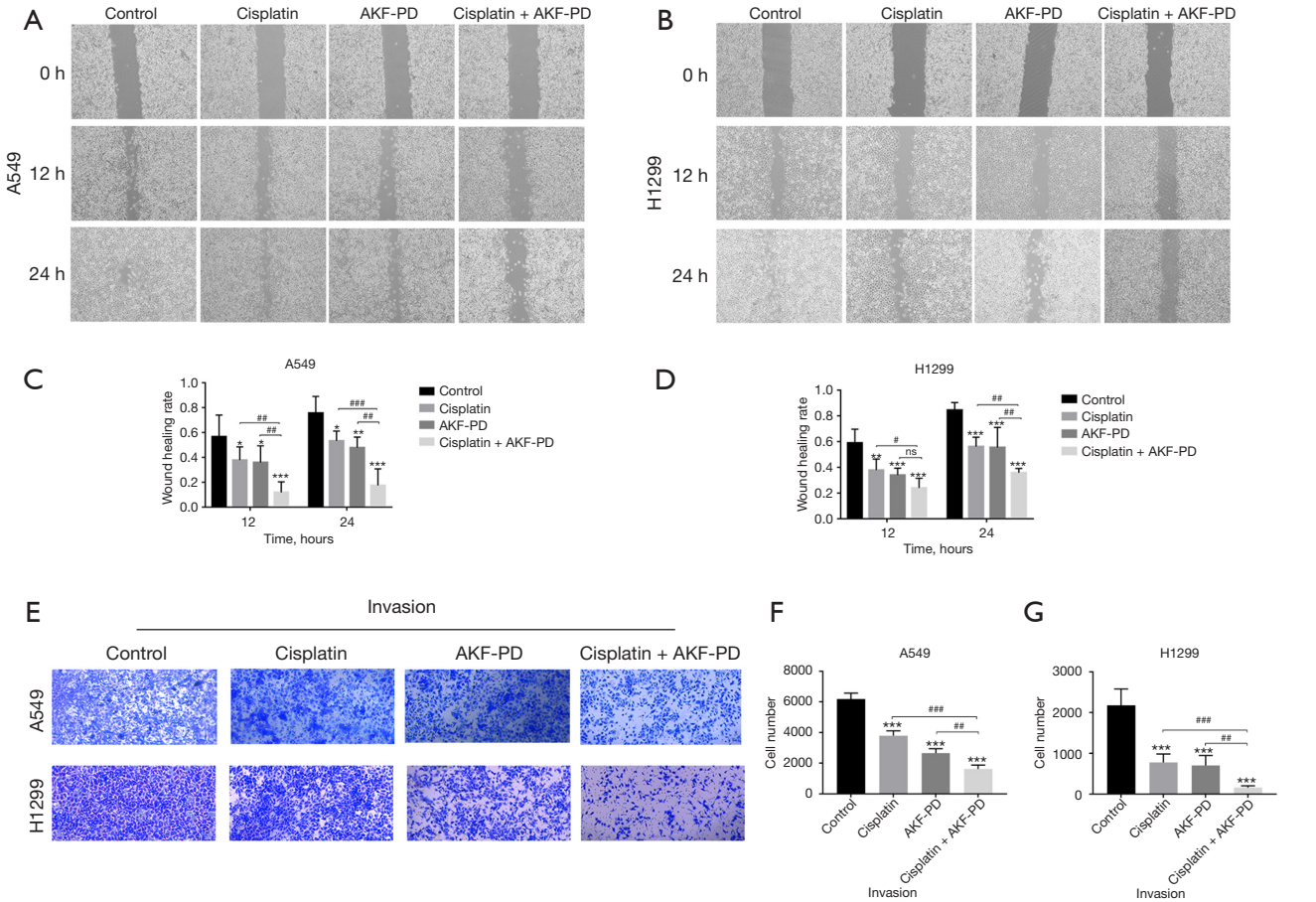

Figure 6 AKF-PD combined with CP yielded increased inhibition of the migration and invasion of NSCLC cells. (A-D) The wound-healing rate of NSCLC cells under the influence with AKF-PD (400 μg/mL) and/or CP (10 μm) was detected by scratch test; magnification: 200×. (E-G) The effects of AKF-PD (400 μg/mL) and/or CP (10 μm) on invasion in the A549 and H1299 cells was determined by Transwell invasion; magnification: 200×; staining: crystal violet. *, P<0.05; **, P<0.01; ***, P<0.001; #, P<0.05; ##, P<0.01; ###, P<0.001; and ns, P>0.05. AKF-PD, fluorofenidone; CP, cisplatin; NSCLC, non-small cell lung cancer.

simultaneously increasing the expression of E-cadherin (*Figure* 7).

AKF-PD combined with CP increased the inhibition of the proliferation of cells of different tumor types

At present, CP is not only the first-line therapy for the treatment of NSCLC, it is also the first-line therapy for the treatment of numerous solid tumors (18). To investigate the effect of the combined treatment of AKF-PD and CP on cells of different tumor types, we used Hela cells, SiHA cells, MDA-MB-231 cells, 5-8F cells, and UM-UC-3 cells. The results were similar to those in NSCLC, i.e., the combination of CP with AKF-PD yielded an increased inhibition of the proliferation of compared to CP alone (Figure S3). These findings suggest that the CP/AKF-PD combination might be a promising therapeutic approach in different tumor types.

Discussion

CP treatment is effective against solid tumors; however, its use is limited due to its significant toxicity, which can cause renal impairment (24). Extensive research has been conducted to determine how to mitigate CP-induced AKI; however, many approaches could potentially reduce also the anti-tumor efficacy of CP (8). In this study, we found that the novel anti-AKI drug AKF-PD directly inhibited the proliferation, invasion, and migration of NSCLC cells, and enhanced the antitumor effect of CP.

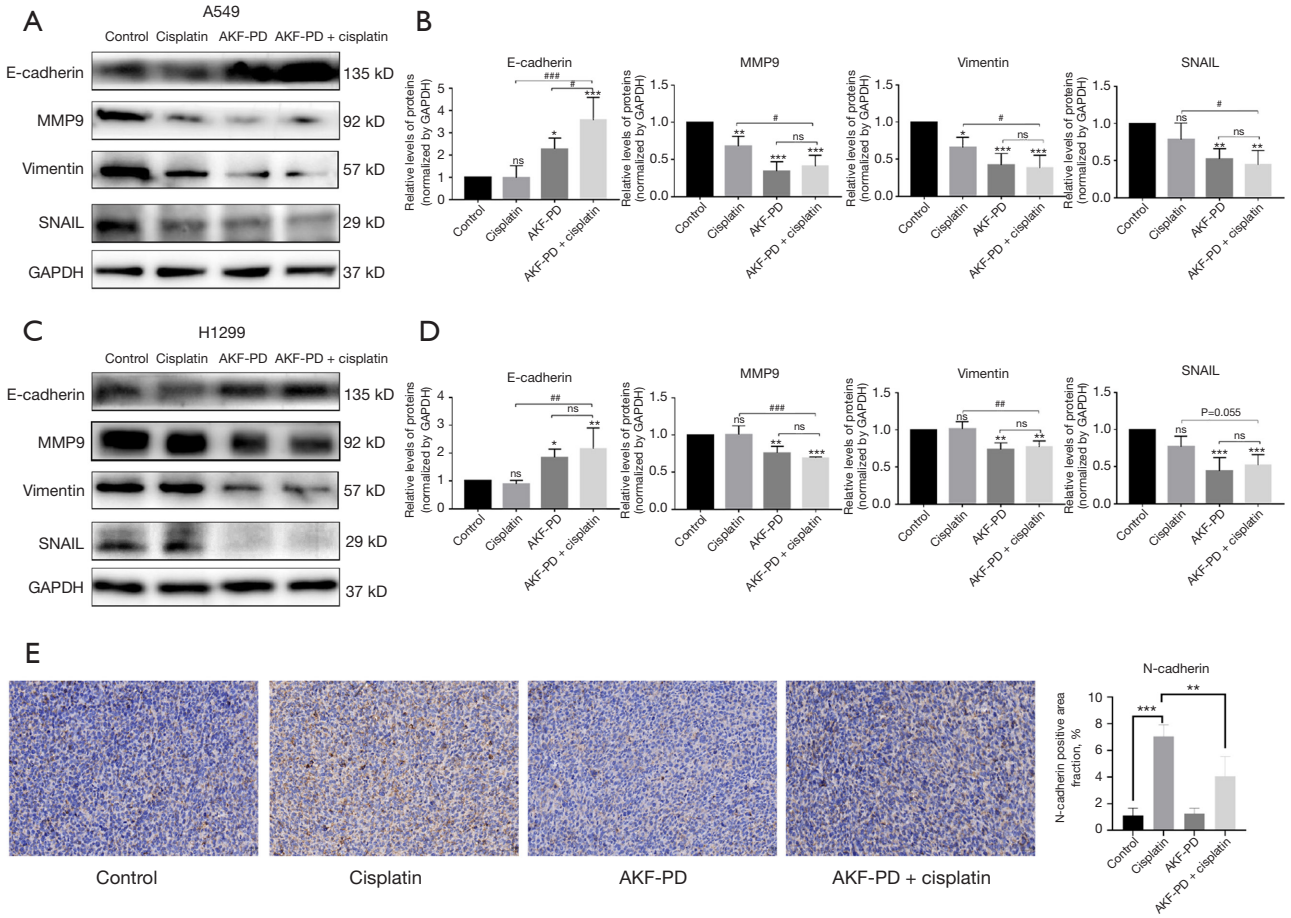

Figure 7 AKF-PD combined with CP yielded increased inhibition of the EMT of NSCLC cells. (A-D) To determine the effect of AKF-PD (400 μg/mL) and/or CP (10 μm) on EMT, the expression and analysis of E-cadherin, MMP9, vimentin, and SNAIL proteins in (A,B) A549 and (C,D) H1299 were detected by western blot. (E) In the *in vivo* study, the effects of AKF-PD (400 mg/kg/d) and/or CP (5 mg/kg) on the expression of N-cadherin were detected by immunohistochemistry in the subcutaneous tumors of mice; magnification: 200×. *, P<0.05; **, P<0.01; ***, P<0.001; #, P<0.05; ##, P<0.01; ###, P<0.001; and ns, P>0.05. AKF-PD, fluorofenidone; E-cadherin, epithelial cadherin; MMP9, matrix metallopeptidase 9; SNAIL, snail family transcriptional repressor 1; GAPDH, glyceraldehyde-3-phosphate dehydrogenase; CP, cisplatin; EMT, epithelial-mesenchymal transition; NSCLC, non-small cell lung cancer.

Recent evidence suggests that pulmonary fibrosis is a significant risk factor in the development of lung cancer (25). Previous studies have shown the efficacy of AKF-PD in treating fibrosis of multiple organs as well as acute organ injuries, in particular pulmonary fibrosis and CP-induced AKI (18,26-28). AKF-PD was found to inhibit the PI3K/Akt/mTOR signaling pathway and promote autophagy, which contributed to the attenuation of paraquat-induced pulmonary fibrosis (29). Thus, prompted us to investigate the possible direct antitumor effect of AKF-PD on NSCLC.

We performed CCK-8 assays, colony-forming assays, EdU assays, cell-scratch tests, and invasion tests to comprehensively evaluate the direct effects of AKF-PD on NSCLC. We found that AKF-PD significantly inhibited, in a dose-dependent manner, the proliferation, invasion, and migration of NSCLC cells.

EMT is a dynamic epigenetic reprogramming event that occurs in a subset of tumor cells, and represents a step promoting cell invasion and distant metastasis (30,31). Moreover, tumor cells that have undergone an EMT gain also malignant features, including stem cell-like features, drug resistance, and immunosuppressive properties (32-34). Here, we evaluated possible EMT-associated phenotypic changes in AKF-PD-treated cells. AKF-PD significantly

increased the expression of epithelial while decreasing the expression of mesenchymal markers *in vitro*. These changes were accompanied by a significant downregulation of the MAPK and PI3K/AKT/mTOR pathways, which are involved in promoting tumor growth and EMT-associated changes (35-37).

As CP remains the first-line option for the treatment of NSCLC and various other cancer types (38), the pursuit of a combined therapeutic approach is a promising strategy to enhance its antitumor efficacy while mitigating adverse effects (39). In the current study, we observed a significant reduction in the EC_{50} value of AKF-PD when combined with CP. Further, the combination of AKF-PD and CP significantly reduced the EMT as compared to that induced by CP alone. Also, from our preliminary observations, the inhibition rate of invasion and migration function compared with the control group was better than that in the proliferation ability at the same dose. These sustain that the above functions may be related to the effect of AKF-PD on EMT. Given that changes in cell numbers may be related not only to proliferation but also to cell death, we also measured cell apoptosis through flow cytometry and found that AKF-PD did not affect the apoptosis of NSCLC. Most importantly, in *in vivo* experiments we showed that AKF-PD could significantly enhance the antitumor activity of CP.

Eventually, we investigated the effects of AKF-PD combined with CP on different tumor cell lines, including cervical carcinoma, nasopharyngeal cancer, triple-negative breast cancer, and bladder cancer cells. The results showed that AKF-PD increased the sensitivity to CP in these cell lines at a dose (400 μg/mL), which had been shown in previous studies to be the maximum dose of AKF-PD that can be used without damaging normal cells and preventing CP-induced AKI (10,40,41). Thus, we recommend this dosage for further preclinical and clinical investigations.

Conclusions

Our results show that AKF-PD can significantly enhance the anti-cancer efficacy of CP. The identification of the molecular target that mediates the antitumor effects of AKF-PD that have been herein described requires further investigations.

Acknowledgments

Funding: This work was supported by the Natural Science Foundation of Hunan Province (No. 2023JJ40828), the Supporting Project for Middle-Aged Scientific and Technological Talents of Qinghai Association for Science and Technology (No. 2021QHSKX RCTJ15), the Qinghai Clinical Research Center for Respiratory Diseases (No. 2019-SF-L4), the National Key Clinical Specialty-Department of Pulmonary and Critical Care Medicine (No. 2023), the Scientific Research Launch Project for New Employees of the Second Xiangya Hospital of Central South University, the Fundamental Research Project of Qinghai Provincial Science and Technology Department (No. 2023-ZJ-782), and the Qinghai Provincial Health Commission (No. 2020-wjzdx-13).

Footnote

Reporting Checklist: The authors have completed the ARRIVE reporting checklist. Available at https://tlcr.amegroups.com/article/view/10.21037/tlcr-24-811/rc

Data Sharing Statement: Available at https://tlcr.amegroups.com/article/view/10.21037/tlcr-24-811/dss

Peer Review File: Available at https://tlcr.amegroups.com/article/view/10.21037/tlcr-24-811/prf

Conflicts of Interest: All authors have completed the ICMJE uniform disclosure form (available at https://tlcr.amegroups.com/article/view/10.21037/tlcr-24-811/coif). F.M. reports that he has received honoraria from ABOCA for the writing of scientific manuscripts in the last 36 months, outside the submitted study. The other authors have no conflicts of interest to declare.

Ethical Statement: The authors are accountable for all aspects of the work in ensuring that questions related to the accuracy or integrity of any part of the work are appropriately investigated and resolved. Animal experiments were performed under a project license (No. 20220493) granted by the Experimental Animal Ethics Committee of the Second Xiangya Hospital of Central South University, in compliance with the Second Xiangya Hospital guidelines for the care and use of animals.

References

1. Siegel RL, Giaquinto AN, Jemal A. Cancer statistics, 2024. CA Cancer J Clin 2024;74:12-49.
2. Sorin M, Prosty C, Ghaleb L, et al. Neoadjuvant Chemoimmunotherapy for NSCLC: A Systematic Review and Meta-Analysis. JAMA Oncol 2024;10:621-33.
3. Wang S, Ma H, Li H, et al. Alternatively Expressed Transcripts Analysis of Non-Small Cell Lung Cancer Cells under Different Hypoxic Microenvironment. J Oncol 2021;2021:5558304.
4. Ghosh S. Cisplatin: The first metal based anticancer drug. Bioorg Chem 2019;88:102925.
5. Friedlaender A, Perol M, Banna GL, et al. Oncogenic alterations in advanced NSCLC: a molecular super-highway. Biomark Res 2024;12:24.
6. Duan Z, Cai G, Li J, et al. Cisplatin-induced renal toxicity in elderly people. Ther Adv Med Oncol 2020;12:1758835920923430.
7. Song Z, Zhu J, Wei Q, et al. Canagliflozin reduces cisplatin uptake and activates Akt to protect against cisplatin-induced nephrotoxicity. Am J Physiol Renal Physiol 2020;318:F1041-52.
8. Hu X, Ma Z, Wen L, et al. Autophagy in Cisplatin Nephrotoxicity during Cancer Therapy. Cancers (Basel) 2021;13:5618.
9. Gu L, He X, Zhang Y, et al. Fluorofenidone protects against acute liver failure in mice by regulating MKK4/JNK pathway. Biomed Pharmacother 2023;164:114844.
10. Song C, He L, Zhang J, et al. Fluorofenidone attenuates pulmonary inflammation and fibrosis via inhibiting the activation of NALP3 inflammasome and IL-1β/IL-1R1/MyD88/NF-κB pathway. J Cell Mol Med 2016;20:2064-77.
11. Wang LH, Liu JS, Ning WB, et al. Fluorofenidone attenuates diabetic nephropathy and kidney fibrosis in db/db mice. Pharmacology 2011;88:88-99.
12. Yuan Q, Wang R, Peng Y, et al. Fluorofenidone attenuates tubulointerstitial fibrosis by inhibiting TGF-β(1)-induced fibroblast activation. Am J Nephrol 2011;34:181-94.
13. Peng Y, Yang H, Wang N, et al. Fluorofenidone attenuates hepatic fibrosis by suppressing the proliferation and activation of hepatic stellate cells. Am J Physiol Gastrointest Liver Physiol 2014;306:G253-63.
14. Tzouvelekis A, Karampitsakos T, Gomatou G, et al. Lung cancer in patients with Idiopathic Pulmonary Fibrosis. A retrospective multicenter study in Greece. Pulm Pharmacol Ther 2020;60:101880.
15. Tzouvelekis A, Gomatou G, Bouros E, et al. Common Pathogenic Mechanisms Between Idiopathic Pulmonary Fibrosis and Lung Cancer. Chest 2019;156:383-91.
16. Hamoir C, Horsmans Y, Stärkel P, et al. Risk of hepatocellular carcinoma and fibrosis evolution in hepatitis C patients with severe fibrosis or cirrhosis treated with direct acting antiviral agents. Acta Gastroenterol Belg 2021;84:25-32.
17. Cox TR, Erler JT. Molecular pathways: connecting fibrosis and solid tumor metastasis. Clin Cancer Res 2014;20:3637-43.
18. Jiang Y, Quan J, Chen Y, et al. Fluorofenidone protects against acute kidney injury. FASEB J 2019;33:14325-36.
19. Xiao J, Zhou N, Li Y, et al. PEITC inhibits the invasion and migration of colorectal cancer cells by blocking TGF-β-induced EMT. Biomed Pharmacother 2020;130:110743.
20. Xu E, Xia X, Jiang C, et al. GPER1 Silencing Suppresses the Proliferation, Migration, and Invasion of Gastric Cancer Cells by Inhibiting PI3K/AKT-Mediated EMT. Front Cell Dev Biol 2020;8:591239.
21. Liu K, Hu H, Jiang H, et al. RUNX1 promotes MAPK signaling to increase tumor progression and metastasis via OPN in head and neck cancer. Carcinogenesis 2021;42:414-22.
22. Xu W, Yu M, Qin J, et al. LACTB Regulates PIK3R3 to Promote Autophagy and Inhibit EMT and Proliferation Through the PI3K/AKT/mTOR Signaling Pathway in Colorectal Cancer. Cancer Manag Res 2020;12:5181-200.
23. Ning WB, Hu GY, Peng ZZ, et al. Fluorofenidone inhibits Ang II-induced apoptosis of renal tubular cells through blockage of the Fas/FasL pathway. Int Immunopharmacol 2011;11:1327-32.
24. Hama T, Nagesh PK, Chowdhury P, et al. DNA damage is overcome by TRIP13 overexpression during cisplatin nephrotoxicity. JCI Insight 2021;6:e139092.
25. Hata A, Nakajima T, Matsusaka K, et al. Genetic alterations in squamous cell lung cancer associated with idiopathic pulmonary fibrosis. Int J Cancer 2021;148:3008-18.
26. Tu S, Jiang Y, Cheng H, et al. Fluorofenidone protects liver against inflammation and fibrosis by blocking the activation of NF-κB pathway. FASEB J 2021;35:e21497.
27. Liao X, Jiang Y, Dai Q, et al. Fluorofenidone attenuates renal fibrosis by inhibiting the mtROS-NLRP3 pathway

in a murine model of folic acid nephropathy. Biochem Biophys Res Commun 2021;534:694-701.
28. Tang Y, Li B, Wang N, et al. Fluorofenidone protects mice from lethal endotoxemia through the inhibition of TNF-alpha and IL-1beta release. Int Immunopharmacol 2010;10:580-3.
29. Jiang F, Li S, Jiang Y, et al. Fluorofenidone attenuates paraquat-induced pulmonary fibrosis by regulating the PI3K/Akt/mTOR signaling pathway and autophagy. Mol Med Rep 2021;23:405.
30. Konen JM, Rodriguez BL, Padhye A, et al. Dual Inhibition of MEK and AXL Targets Tumor Cell Heterogeneity and Prevents Resistant Outgrowth Mediated by the Epithelial-to-Mesenchymal Transition in NSCLC. Cancer Res 2021;81:1398-412.
31. Korpal M, Lee ES, Hu G, et al. The miR-200 family inhibits epithelial-mesenchymal transition and cancer cell migration by direct targeting of E-cadherin transcriptional repressors ZEB1 and ZEB2. J Biol Chem 2008;283:14910-4.
32. Manshouri R, Coyaud E, Kundu ST, et al. ZEB1/NuRD complex suppresses TBC1D2b to stimulate E-cadherin internalization and promote metastasis in lung cancer. Nat Commun 2019;10:5125.
33. Romeo E, Caserta CA, Rumio C, et al. The Vicious Cross-Talk between Tumor Cells with an EMT Phenotype and Cells of the Immune System. Cells 2019;8:460.
34. Marcucci F, Stassi G, De Maria R. Epithelial-mesenchymal transition: a new target in anticancer drug discovery. Nat Rev Drug Discov 2016;15:311-25.
35. Ma Y, Nenkov M, Schröder DC, et al. Fibulin 2 Is Hypermethylated and Suppresses Tumor Cell Proliferation through Inhibition of Cell Adhesion and Extracellular Matrix Genes in Non-Small Cell Lung Cancer. Int J Mol Sci 2021;22:11834.
36. Li Q, Qin T, Bi Z, et al. Rac1 activates non-oxidative pentose phosphate pathway to induce chemoresistance of breast cancer. Nat Commun 2020;11:1456.
37. Jiang Y, Xie F, Lv X, et al. Mefunidone ameliorates diabetic kidney disease in STZ and db/db mice. FASEB J 2021;35:e21198.
38. Cui Z, Li D, Zhao J, et al. Falnidamol and cisplatin combinational treatment inhibits non-small cell lung cancer (NSCLC) by targeting DUSP26-mediated signal pathways. Free Radic Biol Med 2022;183:106-24.
39. Hu Y, Xu Y, Zhang T, et al. Cisplatin-activated ERβ/DCAF8 positive feedback loop induces chemoresistance in non-small cell lung cancer via PTEN/Akt axis. Drug Resist Updat 2023;71:101014.
40. Qin J, Mei WJ, Xie YY, et al. Fluorofenidone attenuates oxidative stress and renal fibrosis in obstructive nephropathy via blocking NOX2 (gp91phox) expression and inhibiting ERK/MAPK signaling pathway. Kidney Blood Press Res 2015;40:89-99.
41. Liu W, Zhou H, Dong H, et al. Fluorofenidone Attenuates Renal Interstitial Fibrosis by Enhancing Autophagy and Retaining Mitochondrial Function. Cell Biochem Biophys 2023;81:777-85.

Cite this article as: Wang S, Liu G, Yu L, Zhang C, Marcucci F, Jiang Y. Fluorofenidone enhances cisplatin efficacy in non-small cell lung cancer: a novel approach to inhibiting cancer progression. Transl Lung Cancer Res 2024;13(11):3175-3188. doi: 10.21037/tlcr-24-811